arXiv:astro-ph/0410672v1 27 Oct 2004

Submitted to ApJL

Rotation Velocities of Two Low Luminosity Field Galaxies

James Pizagno[1], Michael R. Blanton[2], David H. Weinberg[1], Neta A. Bahcall[3], Jon Brinkmann[4]

ABSTRACT

We present Hα rotation curves of two low luminosity field galaxies with r-band absolute magnitudes $M_r = -13.9^{+0.8}_{-0.5}$ and $M_r = -14.7^{+0.3}_{-0.2}$ (for $h \equiv H_0/100\,\mathrm{km\,s^{-1}\,Mpc^{-1}} = 0.7$; the large error bars reflect distance uncertainties). Most previously studied galaxies in this luminosity range are members of groups defined by brighter galaxies, but these two systems, selected from Blanton et al.'s (2004) sample of low luminosity galaxies in the Sloan Digital Sky Survey (SDSS), appear to have no bright companions. The measured rotation speeds at the outer extent of the Hα rotation curves, $34.8\pm3.8\,\mathrm{km\,s^{-1}}$ and $30.9\pm7.2\,\mathrm{km\,s^{-1}}$, are larger than the values of $16.0^{+6.1}_{-5.4}\,\mathrm{km\,s^{-1}}$ and $20.9^{+6.2}_{-5.2}\,\mathrm{km\,s^{-1}}$ predicted by extrapolating the inverse Tully-Fisher relation of luminous SDSS galaxies to these faint luminosities. However, a previous HI measurement of the first galaxy shows that it has a gas mass similar to its stellar mass, and the total baryonic mass is consistent with that predicted by McGaugh et al.'s (2000) "baryonic Tully-Fisher relation." We find r-band dynamical mass-to-light ratios within the radii of the last Hα data points (about 1.8 disk scale lengths in each case) of $12.6^{+4.7}_{-4.5}\,M_\odot/L_\odot$ and $4.8^{+2.5}_{-2.1}\,M_\odot/L_\odot$, much higher than the values $\sim 1\,M_\odot/L_\odot$ expected for the stellar populations. The dynamical properties of these galaxies, including the rotation speeds and evidence for high gas fractions and dark matter domination within the luminous extent of the galaxy, are consistent with those of previously studied faint galaxies in nearby groups. Further studies of the SDSS sample will allow characterization of low luminosity galaxies over the full range of environments in which they reside.

Subject headings: galaxies: photometry, kinematics and dynamics

[1]Department of Astronomy, Ohio State University, Columbus, OH 43210

[2]Department of Physics, New York University, New York, NY 10003

[3]Princeton University Observatory, Princeton, NJ 08544

[4]Apache Point Observatory, 2001 Apache Point Road, P.O. Box 59, Sunspot, NM 88349-0059

1. Introduction

The Sloan Digital Sky Survey (York et al. 2000) galaxy redshift survey has an unprecedented combination of large area, depth, and photometric quality, thanks to the combination of a large format camera (Gunn et al. 1998), high throughput multi-object spectrographs (A. Uomoto et al., in preparation), careful calibration procedures (Fukugita et al. 1996; Hogg et al. 2001; Smith et al. 2002), and an efficient series of data reduction and targeting pipelines (Lupton et al. 2001; Stoughton et al. 2002; Strauss et al. 2002; Blanton et al. 2003a; Pier et al. 2003). Recently Blanton et al. (2004a, hereafter B04) have searched the SDSS Second Data Release (DR2; Abazajian et al. 2004a) to identify a population of extremely low luminosity field galaxies. With absolute magnitudes $M_r \sim -13$ to -16 (for the Hubble parameter $h \equiv H_0/100\,\mathrm{km\,s^{-1}\,Mpc^{-1}} = 0.7$ adopted throughout this paper), this population represents a range of luminosities that has previously been accessible to systematic study only in the Local Group and in nearby groups and clusters.[1] We have obtained Hα rotation curves of two of these objects, using the same methods that we are using for a study of the Tully-Fisher (1977, hereafter TF) relation of more luminous SDSS galaxies (J. Pizagno et al., in preparation, hereafter P04). Both objects appear to be "field" galaxies rather than satellites of brighter systems. Although the sample is small and the data quality limited, these measurements provide one of the first insights into the dynamical properties of this new population.

2. Observations

The galaxies in this paper were selected from the B04 sample according to their availability during an observing run for the P04 project. As detailed in B04 and Blanton et al. (2004b), this low luminosity galaxy sample has been checked for contamination by double stars, errors in the photometric pipeline's automated deblending, and other complications that are unimportant for the great majority of SDSS galaxies but have a significant impact for low luminosity and low redshift systems. The two galaxies selected for follow-up observations were J123654.9+013654.2 and J091858.60+581407.7. For brevity, we will hereafter refer to these as Galaxy 1 and Galaxy 2, respectively.

Distances for galaxies in the B04 sample are estimated from their redshifts assuming Hubble flow and a model for the local peculiar field based on the IRAS 1.2-Jy redshift survey

[1]The field galaxy survey of Schombert, Pildis, & Eder (1997), based on visual inspection of POSS-II plates and HI confirmation from Arecibo, includes some systems in this luminosity range.

(Willick et al. 1997). Details of this procedure are described by Blanton et al. (2004b). Because these galaxies have low redshifts (heliocentric values of $594\,\mathrm{km\,s^{-1}}$ and $1157\,\mathrm{km\,s^{-1}}$, respectively), peculiar velocity uncertainties dominate the distance uncertainties, which in turn dominate the uncertainties in luminosity and dynamically inferred mass-to-light ratios in our discussions below. The Blanton et al. (2004b) procedure yields distances of $9.9 \pm 2.9\,\mathrm{Mpc}$ and $20.0 \pm 2.2\,\mathrm{Mpc}$ to Galaxies 1 and 2, for $h = 0.7$. The 1σ error bars are derived from the peculiar velocity probability function, which includes a $150\,\mathrm{km\,s^{-1}}$ local dispersion around the smooth velocity field predicted from the IRAS 1.2-Jy galaxies. The corresponding Petrosian r-band absolute magnitudes are $M_r = -13.9^{+0.8}_{-0.5}$ and $M_r = -14.7^{+0.3}_{-0.2}$ (again for $h = 0.7$). Neither galaxy has a bright neighbor ($M_r < -19.25$) within 0.7 Mpc projected separation and $1000\,\mathrm{km\,s^{-1}}$ redshift separation. Galaxy 1 is close to NGC 4536 in projection, but the redshift difference, $594\,\mathrm{km\,s^{-1}}$ vs. $1808\,\mathrm{km\,s^{-1}}$ (Grogin, Geller, & Huchra 1998), makes a physical association unlikely. We conclude that both of these objects are "field" galaxies rather than satellites of brighter parents.

Table 1 lists the magnitudes, redshifts, and distances for Galaxies 1 and 2 along with the $g-r$ colors and axis ratios, exponential disk scale lengths, and rotation speed parameters described below. The top panels of Figure 1 show i-band images from the SDSS. A search through the NASA Extragalactic Database (NED) shows an HI observation (from Matthews & van Driel 2000) for the galaxy FGC 1475, which can be identified as our Galaxy 1 on the basis of angular proximity ($12''$ difference between the NED and SDSS positions), similar axis ratios, and similarity between the Matthews & van Driel (2000) and SDSS redshifts.

Spectroscopic observations were made with the CCDS long-slit spectrograph, set up to observe redshifted Hα, at the 2.4 meter MDM telescope during the night of 13 April 2004. We used a $2''$ slit width with a 600 lines/mm grating in the second order producing a 0.41 Å/pixel dispersion, and a $0.41\,''$/pixel spatial scale. The seeing during the night was $1.4-2''$.

The Hα emission lines typically had a total signal-to-noise ratio of $6-15$, with an intensity weighted velocity centroid uncertainty of ~ 8 km/sec. The dispersion axis was aligned to be perpendicular to the columns of the CCD to an accuracy of 0.1Å, as judged from the telluric lines. This alignment ensures that the Hα recession velocity is measured to the accuracy of the intensity weighted velocity centroids. The details of the data reduction and rotation curve extraction can be found in P04.

The bottom panels of Figure 1 show the linearized and flat-fielded spectra of both galaxies. Figure 2 presents the extracted rotation curve measurements as observed velocity relative to the continuum center vs. position along the slit in arc-seconds. Following Courteau (1997) and P04, we fit the rotation curve measurements with an arc-tangent function, which has a minimal number of free parameters while still describing the global shape

of typical galaxy rotation curves quite well. Specifically, we use a Levenburg-Marquardt χ^2 minimization routine (Press et. al. 1992) to fit the data with the functional form

$$V(r) = V_0 + \frac{2}{\pi} V_{\rm circ} \arctan\left(\frac{r - r_0}{r_t}\right), \tag{1}$$

where V_0 is the central velocity, $V_{\rm circ}$ is the asymptotic circular velocity, r is the position along the slit, r_0 is the center of the rotation curve (where $V = V_0$), and r_t is the turnover radius at which the rotation curve begins to flatten. The parameter uncertainties are derived from the covariance matrix returned by the Levenburg-Marquardt routine. For Galaxy 1, we allow all four parameters (V_0, $V_{\rm circ}$, r_0, r_t) to vary. For Galaxy 2, the best-fit arc-tangent parameters have very large $V_{\rm circ}$ and r_t, so that they effectively describe a straight line over the region covered by the data points. We therefore fit a straight line to the rotation curve instead of an arc-tangent function, simplifying the determination of best-fit parameters and uncertainties. Since Galaxy 2's rotation curve is more extended on one side, we fix the line's intercept such that the line goes through the location of the conintuum center at the center of mass velocity.

Figure 2 shows the arc-tangent and linear fits to the data points as smooth solid curves. For Galaxy 1, the outermost data points probe the turnover region of the rotation curve, while for Galaxy 2 they are still linearly rising. Clearly these data do not yield good constraints on the asymptotic circular velocity of a flat rotation curve. However, we find in P04 that the velocity $V_{\rm end}$ defined by the value of the arc-tangent fit at the radius of the outermost data point often provides a useful measurement of rotation speed even when the observed rotation curve is still rising at this radius. In particular, we find that if we use $V_{\rm end}$ as the measure of rotation speed in the TF relation, then the observed TF scatter does not increase significantly when we include galaxies that have rising rotation curves in the sample. While the value of $V_{\rm end}$ is a lower limit to the asymptotic circular velocity, it can be much more robustly measured than $V_{\rm circ}$ from truncated rotation curves like those in Figure 2.

We correct $V_{\rm end}$ for inclination by using the GALFIT program (Peng et. al. 2002) to fit inclined exponential disks to the i-band galaxy images shown in Figure 1. The disk axis ratios and exponential scale lengths are listed in Table 1; formal uncertainties are ~ 0.01 in b/a and $\sim 0.3''$ in $R_{\rm exp}$, though the systematic errors associated with assuming an exponential disk model are probably larger. The inclination corrected velocity is

$$V^i_{\rm end} = V_{\rm end} \left(\frac{1 - b^2/a^2}{1 - 0.19^2}\right)^{-1/2}, \tag{2}$$

where 0.19 is the assumed intrinsic axis ratio for an edge-on disk and b/a is the measured i-band axis ratio. Different ranges for the intrinsic axis ratio vary by 0.10 to 0.20 depending

on galaxy type (Haynes & Giovanelli 1984). We chose 0.19, typical for spiral galaxies, and note that the range in intrinsic axis ratios causes a small variation (typically $\sim$1 km s^{-1}) in $V^i_{\rm end}$. GALFIT yields a position angle for Galaxy 2 that differs from the SDSS DR2 value by ten degrees, consistent with the visual impression of slight misalignment in Figure 1. We therefore apply a small ($\sim 1\,{\rm km\,s^{-1}}$) correction to the measured $V_{\rm end}$ assuming a tilted-ring model as described by Beauvais & Bothun (2001; see their eq. 3). Table 1 lists inclination-corrected values $V^i_{\rm end}$ including this slit misalignment correction for Galaxy 2.

Matthews & van Driel (2000) report an HI velocity width for Galaxy 1 of $W_{50,c} = 94\,{\rm km\,s^{-1}}$, where the subscript c indicates a correction for instrumental resolution. They do not give an error bar on $W_{50,c}$, though the total signal-to-noise ratio of the HI line is 4.8, so the uncertainty in the width is probably not negligible. Kannappan, Fabricant, & Franx (2002) compare HI linewidths to optically measured, maximum rotation speeds and report a correlation

$$W_{50} = 19(\pm 6) + 0.90(\pm 0.03)(2V_{\rm max}) \ , \tag{3}$$

in km s^{-1} units. Equation (3) predicts $V_{\rm max} = 42 \pm 5\,{\rm km\,s^{-1}}$, compared to our measured value of $V_{\rm end} = 34.8 \pm 3.8\,{\rm km\,s^{-1}}$. (Note that the inclination correction is negligible for this galaxy.) The two measurements thus appear to be consistent within the observational errors (allowing for a few percent uncertainty in the measured $W_{50,c}$), though the somewhat higher value inferred from the HI data could reflect a continuing rise of the rotation curve beyond the radius probed by our Hα measurements.

3. Discussion

How do our measured rotation speeds compare to expectations based on the TF relation defined by more luminous galaxies? In P04, we use a sample of 170 galaxies with $-22 < M_r < -18$ to measure the forward (M vs. $\log V$) and inverse ($\log V$ vs. M) TF relations in the SDSS bands. For the r-band inverse relation, we fit

$$\eta = a(M_r - M_{r,0}) + b \tag{4}$$

with $\eta \equiv \log_{10} V^i_{\rm end}$ and the constant $M_{r,0} = -20.873$ chosen to yield minimal correlation between the errors in a and b. We find $a = -0.143 \pm 0.018$ and $b = 2.202 \pm 0.004$, yielding predicted values of $V^i_{\rm end}$ for Galaxies 1 and 2 of $V_{\rm pred} = 16.0^{+6.1}_{-5.4}\,{\rm km\,s^{-1}}$ and $V_{\rm pred} = 20.9^{+6.2}_{-5.2}\,{\rm km\,s^{-1}}$, respectively. The uncertainties in M_r and in the TF slope both contribute significantly to the errors on $V_{\rm pred}$, and both contributions are non-linear. We have computed upper 1σ error bars by separately varying M_r by -1σ and a by $+1\sigma$ and adding the corresponding values of $\delta V_{\rm pred}$ in quadrature; we follow an analogous procedure for the

lower 1σ error bar. The predicted rotation speeds are well below the measured values of $34.8 \pm 3.8\,\mathrm{km\,s^{-1}}$ and $30.9 \pm 7.2\,\mathrm{km\,s^{-1}}$, though marginally compatible in the latter case because of the large observational errors. Dotted curves in Figure 2 show rotation curves with the same parameters as the solid curves but scaled by $(V_{\rm pred}/V^i_{\rm end})$. Despite the uncertainties in the measurements, it is clear that the galaxies are rotating substantially faster than predicted by an extrapolation of the inverse TF relation to these faint magnitudes. To match the observed rotation speeds while maintaining the P04 normalization at $M_r \approx -21$ would require an inverse TF slope of $a \approx -0.1$, compared to the slope of -0.143 measured in the bright galaxy regime.

We can use our measurements to estimate dynamical mass-to-light ratios within the radius of the outermost Hα data point in each galaxy. We use the simple mass estimator

$$M = \frac{(V^i_{\rm end})^2 R_{\rm end}}{G} \ , \tag{5}$$

ignoring possible corrections for asymmetric drift or non-circular motions, which would be small compared to our observational error bars. The values of $R_{\rm end}$ are 19 and 11 arc-seconds for Galaxies 1 and 2, respectively, corresponding to 1.7 and 1.8 times the exponential scale lengths measured by GALFIT. At our estimated distances of 9.9 ± 2.9 Mpc and 20 ± 2.2 Mpc, the physical values of $R_{\rm end}$ are 0.91 ± 0.27 kpc (Galaxy 1) and 1.07 ± 0.12 kpc (Galaxy 2). We measure the fraction of r-band light within $R_{\rm end}$ for each galaxy and correct the values of M_r in Table 1 accordingly, by 0.24 and 0.14 magnitudes. We do not apply any internal extinction corrections. Adopting $M_{r,\odot} = 4.67$, we find $M/L = 12.6^{+4.7}_{-4.5}\,M_\odot/L_\odot$ for Galaxy 1 and $4.8^{+2.5}_{-2.1}\,M_\odot/L_\odot$ for Galaxy 2. Because $M/L \propto V^2_{\rm end}/d$ and the fractional uncertainties in these quantities are substantial, we compute the upper 1σ error bar by separately varying d by -1σ and $V_{\rm end}$ by $+1\sigma$ and adding the two changes δM in quadrature, and we follow an analogous procedure for the lower 1σ error bar. The M/L value for Galaxy 1 is much higher than the value $\sim 1.3 M_\odot/L_\odot$ expected for a stellar population with the observed $g-r$ color of the galaxy (Bell et al. 2003), so this system is strongly dominated by dark matter within $R_{\rm end}$. The case for dark matter domination in Galaxy 2 is less clear because of the large uncertainty in M/L, though the central value again corresponds to a large ratio of dark matter to stellar mass within $R_{\rm end}$. (The Bell et al. [2003] models imply a stellar mass-to-light ratio of $\sim 0.9 M_\odot/L_\odot$ for Galaxy 2's $g-r$ color.) While all disk galaxies become dark matter dominated at sufficiently large radii, these low luminosity systems appear to have high dark matter fractions even within two disk scale lengths.

To put our measurements in the context of previous results, Figure 3 plots inclination corrected circular velocities against B-band absolute magnitude for our galaxies (filled circles with error bars) and for galaxies with HI line widths and $M_B \gtrsim -15$ from Coté, Carignan, & Freeman (2000; open squares), Begum & Chengalur (2004; open circles), and HI line

widths from Carignan & Freeman (1988; open triangle). For our galaxies, we use $V_{\rm end}^i$ as the indicator of circular velocity, and we convert the (AB) g-band luminosity to the (Vega) B-band luminosity using the galaxy $g-r$ color and $M_B = M_g + 0.365 + 0.46[(g-r) - 0.78]$, obtained using the K-correction code of Blanton et al. (2003b). For Coté, Carignan, & Freeman (2000) we use the value of V_c listed in their tables, and for Begum & Chengalur (2004) and Carignan & Freeman (1988) we estimate V_c visually from the plotted rotation curves. We have not attempted to put observational error bars on the literature data points because this would require a detailed assessment of the uncertainties in the distance measurements, which use a somewhat different method in each case. Coté, Carignan, & Freeman (2000) observe galaxies in the Sculptor and Centaurus A groups and assign group distances based on a variety of indicators (see Coté et al. 1997 and references therein). Begum & Chengalur (2004) assign both of their galaxies to the NGC 4696 group on the basis of proximity and adopt a distance based on the brightest stars (Huchtmeier et al. 2000). Carignan & Freeman (1988) use a combination of group assignment and brightest stars to infer the distance of DDO 154.

The solid line in Figure 3 shows the B-band inverse TF relation extrapolated to the low luminosity regime. We convert the g-band relation of P04 to B-band using $M_B = M_g + 0.19$, appropriate for a galaxy with $g-r = 0.4$. Dotted lines show relations with the slope varied by $\pm 1\sigma$. For bright galaxies, the intrinsic scatter about the mean relation is 0.07 dex in $\log_{10} V_{\rm end}^i$ (P04), smaller than the 0.1 dex observational error bar on Galaxy 1. As noted earlier (on the basis of r-band data), Galaxy 1 is rotating substantially faster than the extrapolated TF relation predicts, while the large error bar on $V_{\rm end}$ leaves Galaxy 2 marginally consistent with the TF extrapolation. The rotation speed of Galaxy 1 appears reasonably in line with that of the other dwarf galaxies, while the rotation speed of Galaxy 2 is noticeably low, perhaps because the optical rotation curve is still rising steadily at our outermost data point. All of these systems are rotating faster than the TF extrapolation predicts; equivalently, they are fainter than predicted given their rotation speeds.

McGaugh et al. (2000) show that low luminosity galaxies are fainter than predicted by the (forward) TF relation defined by bright galaxies, consistent with the result shown in Figure 3. However, faint galaxies are often gas rich, and they show that adding the gas masses inferred from HI observations to the stellar masses leads to a linear relation between $\log M_{\rm bar}$ and $\log V_c$ over four decades in baryonic mass $M_{\rm bar}$, extending down to a few $\times 10^7 M_\odot$. For our Galaxy 1, Matthews & van Driel (2000) report an HI flux integral of 1.24 Jy km s^{-1}, which implies an HI mass to optical luminosity ratio of $\sim 0.95 M_\odot/L_\odot$ in r-band, or roughly equal mass in neutral gas and stars. This ratio is below the median of $\sim 2 M_\odot/L_\odot$ found (in V-band) by Pildis, Schombert, & Eder (1997), but within the range spanned by their data. Simply doubling the luminosity of Galaxy 1 and thus shifting it rightwards by 0.75 mag in

Figure 3 would not move it onto the P04 inverse TF relation. However, McGaugh et al. (2000) find a steep slope for the (forward) baryonic mass TF relation, and the baryonic mass of $7.5 \times 10^7 M_\odot$ inferred for Galaxy 1 at a distance of 9.9 Mpc agrees respectably with the value $M_{\rm bar} = 30.5(h/0.7)^{-2}(V_c/\,{\rm km\,s^{-1}})^4 M_\odot = 5.3 \times 10^7 M_\odot$ predicted by their fitted relation for $V_c = 35\,{\rm km\,s^{-1}}$, given the substantial error bars on both the predicted and measured values.

The luminosity-velocity relations and mass-to-light ratios of low luminosity galaxies offer clues to the role of supernovae and photoionization in regulating star formation, since these feedback effects are generally expected to be stronger in lower mass halos (see, e.g., Dekel & Silk 1986; Quinn, Katz, & Efstathiou 1996; Thoul & Weinberg 1996; Benson et al. 2002; Somerville 2002). The influence of feedback may be different in galaxies that are central objects of their parent dark matter halos and in galaxies that are satellites in more massive halos — semi-analytic models and hydrodynamic simulations predict systematically different properties for these two populations (Kauffmann, White, & Guiderdoni 1993; Cole et al. 1994; Somerville & Primack 1999; Berlind et al. 2003; Zheng et al. 2004). Most of the very low luminosity galaxies studied to date have been discovered or investigated because they are members of groups or clusters defined by brighter galaxies. The two galaxies studied in this paper are not satellites of bright neighbors, but their properties are roughly in line with those of satellite dwarfs. The B04 sample drawn from the SDSS provides the opportunity to study such faint galaxies in detail over the full range of environments in which they appear. Our present investigation represents a start on this broader program.

JP and DW acknowledge support from NSF Grants AST-0098584 and AST-0407125. We thank Eric F. Bell for useful comments. Funding for the creation and distribution of the SDSS Archive has been provided by the Alfred P. Sloan Foundation, the Participating Institutions, the National Aeronautics and Space Administration, the National Science Foundation, the U.S. Department of Energy, the Japanese Monbukagakusho, and the Max Planck Society. The SDSS Web site is http://www.sdss.org/.

The SDSS is managed by the Astrophysical Research Consortium (ARC) for the Participating Institutions. The Participating Institutions are The University of Chicago, Fermilab, the Institute for Advanced Study, the Japan Participation Group, The Johns Hopkins University, Korean Scientist Group, Los Alamos National Laboratory, the Max-Planck-Institute for Astronomy (MPIA), the Max-Planck-Institute for Astrophysics (MPA), New Mexico State University, University of Pittsburgh, Princeton University, the United States Naval Observatory, and the University of Washington.

REFERENCES

Abazajian, K., et al. 2004a, AJ, 128, 502

Beauvais, C. & Bothun, G. 2001, ApJS, 136, 41

Begum, A. & Chengalur, J. N. 2004, A&A, 424, 509

Bell, E. F., McIntosh, D. H., Katz, N., & Weinberg, M. D. 2003, ApJS, 149, 289

Benson, A. J., Lacey, C. G., Baugh, C. M., Cole, S., & Frenk, C. S. 2002, MNRAS, 333, 156

Berlind, A. A., Weinberg, D. H., Benson, A. J., Baugh, C. M., Cole, S., Davé, R., Frenk, C. S., Jenkins, A., Katz, N., & Lacey, C. G. 2003, ApJ, 593, 1

Blanton, M. R., Lupton, R. H., Maley, F. M., Young, N., Zehavi, I., & Loveday, J. 2003a, AJ, 125, 2276

Blanton, M. R., et al. 2003b, AJ, 125, 2348

Blanton, M. R., et al. 2004a, AJ, submitted, astro-ph/0410164 (B04)

Blanton, M. R., et al. 2004b, AJ, submitted, astro-ph/0410166

Carignan, C. & Freeman, K. C. 1988, ApJ, 332, L33

Cole, S., Aragon-Salamanca, A., Frenk, C. S., Navarro, J. F., & Zepf, S. E. 1994, MNRAS, 271, 781

Coté, S., Carignan, C., & Freeman, K. C. 2000, ApJ, 120, 3027

Coté, S., Freeman, K. C., Carignan, C., & Quinn, P. J. 1997, AJ, 114, 1313

Courteau, S. 1997, AJ, 114, 2402

de Blok, W. J. G., McGaugh, S. S., & Rubin, V. C. 2001, AJ, 122, 2396

Dekel, A., & Silk, J. 1986, ApJ, 303, 39

Fukugita, M., Ichikawa, T., Gunn, J. E., Doi, M., Shimasaku, K., & Schneider, D. P. 1996, AJ, 111, 1748

Grogin, N. A., Geller, M. J., & Huchra, J. 1998 ApJS, 199, 277

Gunn, J. E., et al. 1998, AJ, 116, 3040

Haynes, M. P., & Giovanelli, R. 1984, AJ, 89, 758

Hogg, D. W., Schlegel, D. J., Finkbeiner, D. P., & Gunn, J. E. 2001, AJ, 122, 2129

Huchtmeier, W. K., Karachentsev, I. D., Karachentseva, V. E., & Ehle, M. 2000, A&AS, 141, 469

Kannappan, S. J., Fabricant, D. G., & Franx, M. 2002, AJ, 123, 2358

Kauffmann, G., White, S. D. M., & Guiderdoni, B. 1993, MNRAS, 264, 201

Lupton, R., Gunn, J. E., Ivezić, Ž., Knapp, G. R., Kent, S., & Yasuda, N. 2001, in ASP Conf. Ser. 238, Astronomical Data Analysis Software and Systems X, ed. F. R. Harnden, Jr., F. A. Primini, and H. E. Payne (San Francisco: Astr. Soc. Pac.), p. 269, astro-ph/0101420

Marchesini, D., D'Onghia, Chincarini, G., Firmani, C., Conconi, P., Molinari, E., & Zacchei, A. 2002, ApJ, 575, 801

Matthews, L. D., & van Driel, W. 2000, A&AS, 143, 421

McGaugh, S. S., Schombert, J. M., Bothun, G. D., & de Blok, W. J. G. 2000, ApJ, 533, L99

Peng, C. Y., Ho, L. C., Impey C. D., Rix, H.-W. 2002, AJ, 124, 266

Pier, J. R., Munn, J. A., Hindsley, R. B., Hennessy, G. S., Kent, S. M., Lupton, R. H., & Ivezić, Ž. 2003, AJ, 125, 1559

Pildis, R. A., Schombert, J. M., & Eder, J. 1997, ApJ, 481, 157

Press, W. H., Teukolsky, S. A., Vettering, W. T., & Flannery, B. P. 1992, Numerical Recipes (Cambridge: Cambridge Univ. Press)

Quinn, T., Katz, N., & Efstathiou, G. 1996, MNRAS, 278, L49

Schombert, J. M., Pildis, R. A., & Eder, J. 1997, ApJS, 111, 233

Smith, J. A., et al. 2002, AJ, 123, 2121

Somerville, R. S. 2002, ApJ, 572, L23

Somerville, R. S., & Primack, J. R. 1999, MNRAS, 310, 1087

Stoughton, C., et al. 2002, AJ, 123, 485

Strauss, M.A., et al. 2002, AJ, 124, 1810

Thoul, A. A. & Weinberg, D. H. 1996, ApJ, 465, 608

Tully, R. B., & Fisher, J. R. 1977, A&A, 54, 661

Willick, J. A., Strauss, M. A., Dekel, A., & Kolatt, T. 1997, ApJ, 486, 629

York, D. G. et al. 2000, AJ, 120, 1579

Zheng, Z., Berlind, A. A., Weinberg, D. H., Benson, A. J., Baugh, C. M., Cole, S., Davé, R., Frenk, C. S., Katz, N., & Lacey, C. G. 2004, ApJ, submitted, astro-ph/0408564

This preprint was prepared with the AAS LaTeX macros v5.2.

Table 1. Galaxy Properties

Galaxy	r	$g-r$	cz	$d\,(\mathrm{Mpc})$	M_r	$R_{\mathrm{exp}}\,('')$	b/a	V_{end}	V_{pred}
J123654.9+013654.2	16.11	0.41	594	9.9 ± 2.9	$-13.9^{+0.8}_{-0.5}$	11.2	0.20	34.8 ± 3.8	$16.0^{+6.1}_{-5.4}$
J091858.60+581407.7	16.84	0.31	1157	20.0 ± 2.2	$-14.7^{+0.3}_{-0.2}$	6.2	0.40	30.9 ± 7.2	$20.9^{+6.2}_{-5.2}$

Note. — Velocity units (for cz, V_{end}, and V_{pred}) are $\mathrm{km\,s^{-1}}$. Distances and absolute magnitudes are computed assuming $H_0 = 70\,\mathrm{km\,s^{-1}\,Mpc^{-1}}$, using a model of the local peculiar velocity field as described in the text. All the magnitudes are corrected for Galactic foreground extinction.

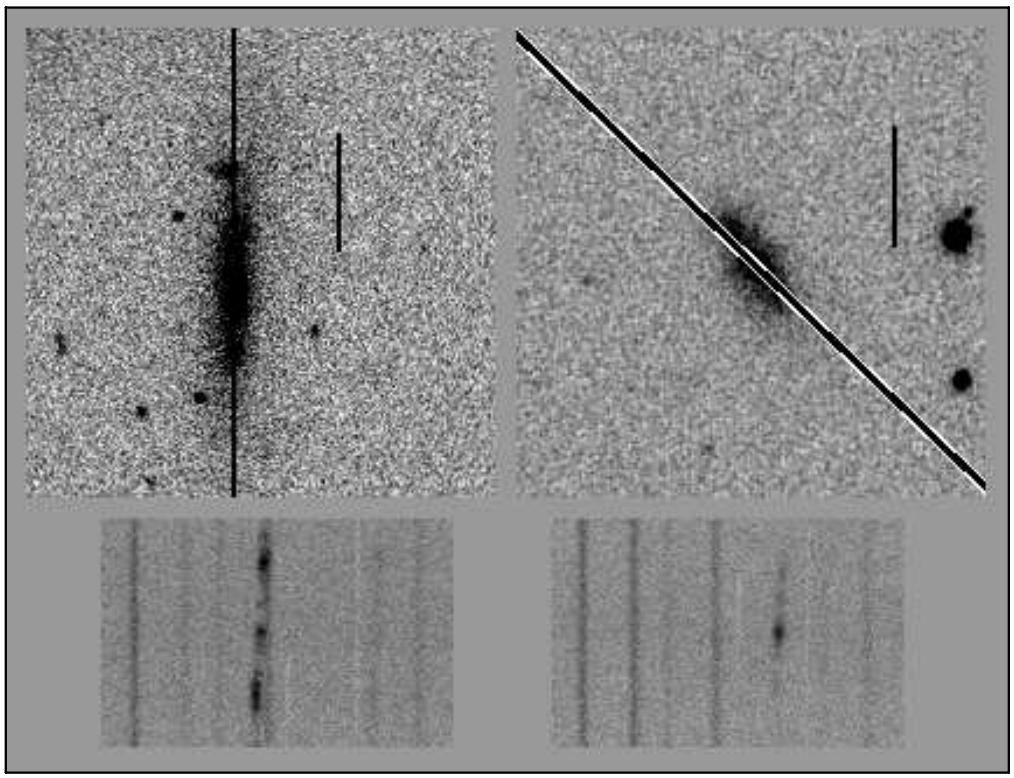

Fig. 1.— Images and spectra of Galaxy 1 (left) and Galaxy 2 (right). Upper panels show the SDSS *i*-band images with North down and East to the left. The small vertical line has a length of 20 arc-seconds, and the long line through each galaxy shows the slit position angle. Lower panels show the flat-fielded, linearized spectra from MDM. These panels are 40 arc-seconds high and 61 Å wide, centered at 6582 Å.

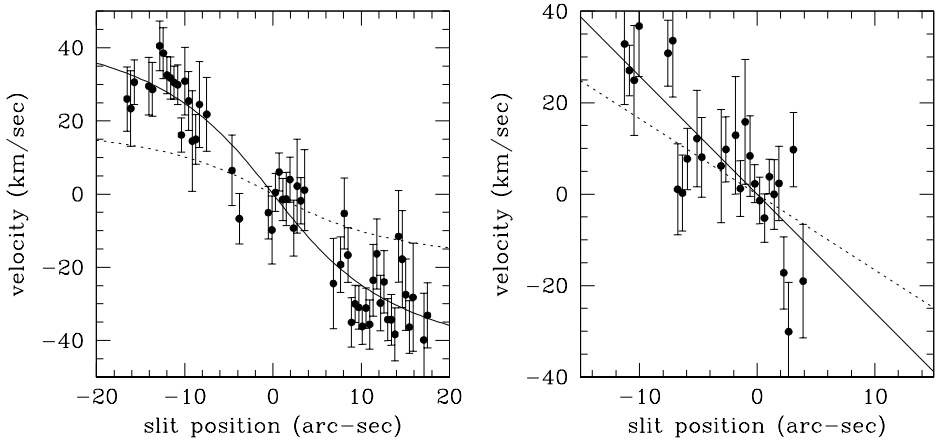

Fig. 2.— Rotation curves of Galaxy 1 (left) and Galaxy 2 (right). Points with error bars show the flux-weighted velocity centroid of the Hα line as a function of position along the slit. For Galaxy 1, the solid curve shows the arc-tangent fit to the data (eq. 1). For Galaxy 2, we use a straight fit. Our measure of circular velocity is the value $V_{\rm end}$ of the smooth fit at the radius of the outermost data point. Dotted curves show the arc-tangent or linear fits scaled by $V_{\rm pred}/V_{\rm end}$, where $V_{\rm pred}$ is the value predicted by extrapolating the inverse TF relation of P04 to the absolute magnitudes of these galaxies. Note that these plots are not corrected for inclination.

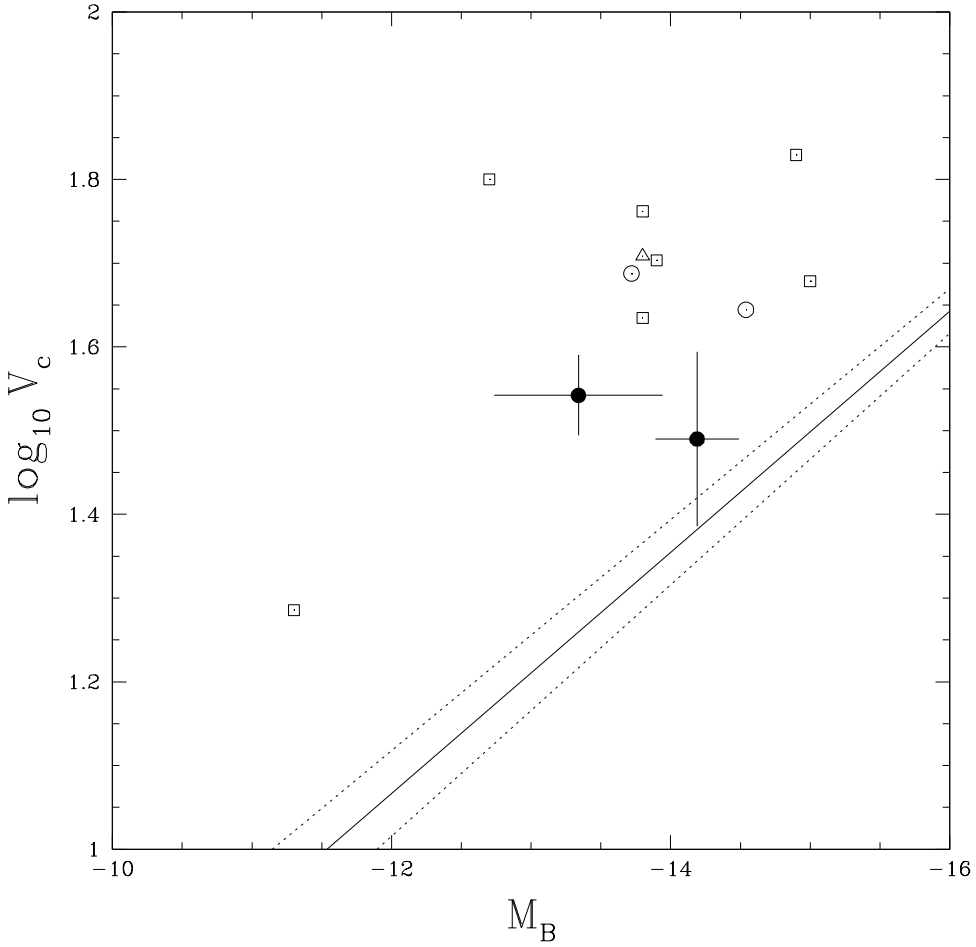

Fig. 3.— Inclination corrected circular velocity vs. B-band absolute magnitude for our galaxies (filled circles with error bars) and for low luminosity galaxies with HI data taken from Coté, Carignan, & Freeman (2000, open squares), Begum & Chengalur (2004, open circles), and Carignan & Freeman (1988, open triangle). The solid line shows the extrapolation of the B-band inverse TF relation to the faint galaxy regime. The B-band inverse TF relation is found by converting the g-band inverse TF relation of P04. Dotted lines show this relation with the slope changed by $\pm 1\sigma$.